

Scientific Article

Plan Assessment Metrics for Dose Painting in Stereotactic Radiosurgery



Benjamin Z. Tham, MSc,^{a,*} Dionne Aleman, PhD,^a Håkan Nordström, PhD,^b Nelly Nygren, MSc,^b and Catherine Coolens, PhD^c

^aDepartment of Mechanical and Industrial Engineering, University of Toronto, Toronto, Ontario, Canada; ^bElekta Instrument AB, Stockholm, Sweden; and ^cDepartment of Radiation Oncology, Princess Margaret Cancer Centre, Toronto, Ontario, Canada

Received 18 October 2022; accepted 23 May 2023

Purpose: As radiation therapy treatment precision increases with advancements in imaging and radiation delivery, dose painting treatment becomes increasingly feasible, where targets receive a nonuniform radiation dose. The high precision of stereotactic radiosurgery (SRS) makes it a good candidate for dose painting treatments, but no suitable metrics to assess dose painting SRS plans exist. Existing dose painting assessment metrics weigh target overdose and underdose equally but are unsuited for SRS plans, which typically avoid target underdose more. Current SRS metrics also prioritize reducing healthy tissue dose through selectivity and dose fall-off, and these metrics assume single prescriptions. We propose a set of metrics for dose painting SRS that would meet clinical needs and are calculated with nonuniform dose painting prescriptions.

Methods and Materials: Sample dose painting SRS prescriptions are first created from Gamma Knife SRS cases, apparent diffusion coefficient magnetic resonance images, and various image-to-prescription functions. Treatment plans are found through semi-infinite linear programming optimization and using clinically determined isocenters, then assessed with existing and proposed metrics. Modified versions of SRS metrics are proposed, including coverage, selectivity, conformity, efficiency, and gradient indices. Quality factor, a current dose painting metric, is applied both without changes and with modifications. A new metric, integral dose ratio, is proposed as a measure of target overdose.

Results: The merits of existing and modified metrics are demonstrated and discussed. A modified conformity index using mean or minimum prescription dose would be suitable for dose painting SRS with integral or maximum boost methods, respectively. Either modified efficiency index is a suitable replacement for the existing gradient index.

Conclusions: The proposed modified SRS metrics are appropriate measures of plan quality for dose painting SRS plans and have the advantage of giving equal values as the original SRS metrics when applied to single-prescription plans.

© 2023 The Author(s). Published by Elsevier Inc. on behalf of American Society for Radiation Oncology. This is an open access article under the CC BY-NC-ND license (<http://creativecommons.org/licenses/by-nc-nd/4.0/>).

Introduction

Dose painting is a radiation therapy treatment method that uses the established heterogeneity of tumor

radiosensitivity to deliver variable prescribed doses. Although dose painting is increasingly being studied in radiation therapy, studies in dose painting radiosurgery are few. In this paper, we investigate assessment metrics

Sources of support: This work was supported by the Elekta AB and Canadian Institutes of Health Research.

Data sharing statement: This work uses anonymized patient data, which was granted access through an ethics board approval. The authors are not permitted to share patient data except in aggregate form (eg, publications).

Corresponding author: Benjamin Z. Tham, MSc; E-mail: benjamin.tham@mail.utoronto.ca

<https://doi.org/10.1016/j.adro.2023.101281>

2452-1094/© 2023 The Author(s). Published by Elsevier Inc. on behalf of American Society for Radiation Oncology. This is an open access article under the CC BY-NC-ND license (<http://creativecommons.org/licenses/by-nc-nd/4.0/>).

for dose painting radiosurgery, setting up a way to quantify plan quality in subsequent studies.

Dose painting by numbers (DPBN) is a highly precise treatment method that uses quantitative imaging to vary prescriptions for individual voxels, and it has been made increasingly feasible by improvements in quantitative imaging, plan optimization, and radiation delivery techniques.^{1–6} Numerous studies have demonstrated both feasibility and clinical benefits of using DPBN to apply heterogeneous dose distributions in radiation therapy.^{4–14} With the voxel-level precision required for DPBN, geometric uncertainty in treatment is a consideration that has been accounted for in other studies through geometric methods¹⁵ and optimization methods.^{1,16,17}

Stereotactic radiosurgery (SRS) is a form of high-precision radiation therapy typically used to treat brain tumors. Current SRS treatments have high resolution imaging as input, pretreatment target localization, and strict patient immobilization to ensure submillimeter precision.^{18–20} SRS also typically involves motion tracking during treatment, such as through the Novalis ExacTrac system^{21–23} or through Gamma Knife's frame- or mask-based high-definition motion management camera system.^{24–32} In addition, brain structures typically have low deformation and movement because of skull rigidity, and it is a common clinical practice to have same-day imaging, planning, and treatment. The ongoing development of SRS hardware and techniques continues to improve its precision and versatility. For example, the CyberKnife S7 system has a higher dose rate of up to 1000 MU per minute,³³ so precision is improved through shortened treatment time and reduced intrafraction movement. The established and improving precision of SRS methods makes the heterogeneity of tumors more readily discerned in imaging and treatment, and so this makes it interesting to study the possibilities of DPBN in SRS treatment.

One may assume that metrics for assessing the quality of dose painting radiation therapy plans would extend to dose painting SRS plans. However, clinical priorities in SRS differ sufficiently from those in typical radiation therapy that existing metrics cannot be easily or directly used to evaluate dose painting plan quality in SRS.

The first key difference of SRS treatment plans from conventional radiation therapy plans is the stronger penalizing of target underdose than overdose. The prescription isodose line for SRS plans, which describes the planned treatment dose relative to the planned maximum target dose,³⁴ is typically between 40% to 60%. This ratio corresponds to the maximum target dose of 167% to 250% of the prescribed dose. As such, despite having a single prescribed dose, target “overdose” is expected, and SRS plan metrics such as coverage index and conformity index only account for underdose.

On the other hand, metrics used in existing dose painting studies, such as quality factor^{8,13,35} and the set of 3 indices (index of achievement, index of hotness, and index of

coldness)³⁶ equally weigh both target overdose and underdose and would be heavily skewed when used with SRS plans. Quality- or Q-volume histogram (QVH)³⁷ and difference volume histogram (Δ VH)¹⁶ plots show the deviation of the planned doses from prescribed doses and are useful replacements for targets' dose volume histogram (DVH) plots and are usable with dose painting SRS plans, but these plots are not as easily comparable as numerical indices.

A second key difference of SRS treatments is the emphasis on reducing dose in healthy tissue. The high doses in the target lead to the benefit of a steeper dose fall-off outside the target,^{20,38} which is particularly crucial in SRS treatments because each treatment fraction has, in general, much higher doses than conventional radiation therapy. SRS metrics such as selectivity index and gradient index (GI) prioritize a reduction of healthy tissue dose but are calculated using a single prescription dose and cannot be directly used for dose painting plans. Using modified versions of these metrics would allow clinicians to use the established understanding of existing metrics.

Methods and Materials

Dose painting treatment plans

Data from 8 patients, previously treated with SRS using Gamma Knife Icon and used in studies of radiation-induced change in biomarkers,^{39,40} were selected under an Research Ethics Board-approved clinical trial based on the availability of accompanying diffusion-weighted imaging magnetic resonance imaging (MRI) images.

Clinical single dose prescriptions ranged between 12 and 24 Gy. In addition to preplanning T1- and T2-weighted MRI, apparent diffusion coefficient images were coregistered to the planning MRI, providing a useful indicator of cellular density and a possible gauge for radiation effectiveness.^{41,42} More details of each case can be found in [Table E1](#).

The exact relationships between image type, tumor radiosensitivity, and clinical prescription are complex. For example, Søvik et al⁴³ and Thorwarth et al⁴ use tumor control probability models to estimate prescribed dose, by respectively relating partial pressure of oxygen to radiosensitivity or [¹⁸F]-fluoromisonidazole tracer retention to radioresistance and finally prescribed dose. Other studies have used a simpler linear relationship between voxel intensity with [¹⁸F]fluoro-deoxy-glucose positron emission tomography imaging, hypoxia, and prescribed dose.^{5,37,44} Whether using tumor control probability models or otherwise, each method makes assumptions to simplify the relationships between image, biology, and prescription, and the optimal prescription function requires further study.^{45,46}

In this research, we generated a variety of dose painting prescriptions using different prescription functions

that are used with pretreatment apparent diffusion coefficient values as a metric of tumor heterogeneity. The use of multiple functions reduces the assumptions made in relating image voxel intensity to prescribed dose, as well as allowing a simulation using alternative image types that indicate different kinds of heterogeneity, such as hypoxia instead of hypercellularity, which would then result in different prescriptions.

Four prescription functions, as developed by Bowen et al,⁴⁵ are used to translate voxel image intensity to prescribed dose: polynomial integral boost, polynomial max boost, sigmoid integral boost, and sigmoid max boost. Polynomial functions include the existing linear prescription functions from other studies, and we extend them by using varying polynomial exponents to account for less direct relationships. Sigmoid functions allow resemblance to possible dose-response functions⁴⁵ and thus incorporate some radiobiological considerations into the prescription. The polynomial exponents of 0.5, 1, or 2 and sigmoid function slopes of 2, 4, or 10, combined with 5 levels of dose boosts each, gives 30 different max boost and 30 integral boost dose painting prescription functions for each case. To reduce variability and increase comparability between the various cases and plans, all plans have a base prescription of 21 Gy.

Treatment plans for treating with a Gamma Knife Icon or Perfexion machine are then obtained using optimization with a semi-infinite linear programming formulation and interior point constraint generation.⁴⁷ The optimization objective terms of quadratic overdose penalties (for both targets and organs at risk) and underdose penalties (for targets) are approximated with linear functions, which are generated procedurally by the interior point constraint generation algorithm. Two common sets of optimization parameters are separately used for small and large target volumes, and the output of each optimization is an optimal radiation treatment plan for the dose painting prescription input. It should be noted that this is not a reflection of clinical practice, where a clinician will tune optimization parameters for each case and prescription to get a desired plan, but the optimization does produce sufficiently high-quality plans to allow us to evaluate plan assessment metrics.

Metrics

A list of terms and abbreviations are summarized in Table 1.

Quality factor (QF)³⁷ is a common metric used in dose painting studies, where the quality (Q) of each voxel is the ratio of planned to prescribed dose. In SRS plans this quantity would be too heavily weighted on overdosing, so to accurately capture SRS priorities, QF_{cold} is introduced, which focuses on underdose. QF_{hot} is also defined for completeness,

as well as QF_{hot,125%} and QF_{hot,150%}. As significant portions of typical SRS targets have above 125% and 150% relative dose, the additional indicators may be useful in dose painting SRS. The related equations for QF are

$$Q_{\text{voxel}} \equiv \text{Planned dose}_{\text{voxel}} / \text{prescribed dose}_{\text{voxel}}$$

$$QF = \frac{1}{n} \sum_{\text{volume}} |Q_{\text{voxel}} - 1|$$

$$QF_{\text{cold}} = \frac{1}{n} \sum_{\text{voxel}} [Q_{\text{voxel}} - 1]^{-}$$

$$QF_{\text{hot}} = \frac{1}{n} \sum_{\text{voxel}} [Q_{\text{voxel}} - 1]^{+}$$

$$QF_{\text{hot,125\%}} = \frac{1}{n} \sum_{\text{voxel}} [Q_{\text{voxel}} - 1.25]^{+}$$

$$QF_{\text{hot,150\%}} = \frac{1}{n} \sum_{\text{voxel}} [Q_{\text{voxel}} - 1.5]^{+}$$

Similar to QF where the relative target dose is considered, integral dose ratio (IDR) is proposed. Where QF quantifies deviation from the planned dose, IDR quantifies the overall relative dose ratio:

$$\text{IDR} = \text{Integral dose of GTV} / \text{integral planned dose of GTV}$$

Coverage index, D_{95%}, and V_{95%}, are common metrics used in evaluating SRS plans with single prescriptions. As these metrics only involve the target voxels, we can easily adapt them by scaling calculations according to individual voxel prescriptions, and we use (*) to identify modified versions.

Coverage index, or target coverage, is defined as the ratio of prescription isodose volume (PIV)_{Target} to gross tumor volume (GTV).³⁴ The change for dose painting is to calculate relative to each voxel's prescription instead of marked volumes based on the typical single prescription. D_{95%} is defined as the minimum dose or absorbed dose to 95% of the target volume,³⁴ and V_{95%} is the fraction of the target volume that receives at least 95% of the prescribed dose. D_{95%*} and V_{95%*} are similarly calculated relative to each voxel's prescription dose instead of using absolute dose. The original and modified formulas for coverage are, where TTV is treated target volume:

$$\text{Coverage} = \text{TTV} / \text{GTV}$$

$$\text{Coverage}^* = \frac{\sum \text{voxels}_{\text{planned dose} \geq \text{prescribed dose}}}{\text{GTV}}$$

Three metrics, selectivity index, GI,⁴⁸ and efficiency index (EI),⁴⁹ consider healthy tissue sparing and thus involve voxels outside the target while using a single value

Table 1 Terms and their descriptions and whether they are used with single prescription plans or dose painting prescription plans

Term	Description	Single prescription	Dose painting
GTV	Target volume	✓	✓
PIV	Volume covered by the prescription isodose line	✓	
PIV _{min} & PIV _{mean}	Volume covered by the minimum and mean prescription isodose line, respectively		✓
PIV _{X%}	Volume covered by the X% prescription isodose line	✓	
PIV _{X%,min} & PIV _{X%,mean}	Volume covered by the X% prescription isodose line for minimum and mean prescriptions, respectively		✓
TTV	Target volume covered by the prescription isodose line	✓	
TTV _{min} & TTV _{mean}	Target volume covered by the minimum and mean prescription isodose lines, respectively		✓
Integral dose	Mean dose for the given volume multiplied by the same volume	✓	✓

Abbreviations: GTV = gross tumor volume; PIV = prescription isodose volume; TTV = treated target volume.

for prescribed dose. Scaling by the individual target voxels' prescribed doses is not possible, so we propose the use of the minimum prescribed dose for conservative measures and mean prescribed dose for a measure that scales proportionally to the overall intended dose. These adjusted metrics are indicated with a min or mean subscript, respectively. EI_{12 Gy}, an option suggested for multiple targets,⁴⁵ is applicable for dose painting without modification. The equations for these indices are

$$\text{Selectivity} = \text{TTV}/\text{PIV}$$

$$\text{Selectivity}_{\min} = \text{TTV}_{\min}/\text{PIV}_{\min}$$

$$\text{Selectivity}_{\text{mean}} = \text{TTV}_{\text{mean}}/\text{PIV}_{\text{mean}}$$

$$\text{GI} = \text{PIV}_{50\%}/\text{PIV}$$

$$\text{GI}_{\min} = \text{PIV}_{50\%,\min}/\text{PIV}_{\min}$$

$$\text{GI}_{\text{mean}} = \text{PIV}_{50\%,\text{mean}}/\text{PIV}_{\text{mean}}$$

$$\text{EI}_{50\%} = \text{Integral dose of GTV}/\text{integral dose of PIV}_{50\%}$$

$$\text{EI}_{50\%,\min} = \text{Integral dose of GTV}/\text{integral dose of PIV}_{50\%,\min}$$

$$\text{EI}_{50\%,\text{mean}} = \text{Integral dose of GTV}/\text{integral dose of PIV}_{50\%,\text{mean}}$$

$$\text{EI}_{12 \text{ Gy}} = \text{Integral dose of GTV}/\text{integral dose of PIV}_{12 \text{ Gy}}$$

Paddick conformity index (PCI) is a common metric used to express conformity of dose to the target and can be expressed as a product of coverage index and selectivity index.^{34,50} As we have new definitions for both indices, 2

dose painting–specific PCI formulas can be likewise defined as follows:

$$\begin{aligned} \text{PCI} &= \text{TTV}^2/(\text{GTV} \times \text{PIV}) \\ &= \text{Coverage} \times \text{selectivity} \end{aligned}$$

$$\text{PCI}_{\min}^* = \text{Coverage}^* \times \text{selectivity}_{\min}$$

$$\text{PCI}_{\text{mean}}^* = \text{Coverage}^* \times \text{selectivity}_{\text{mean}}$$

Results

An example optimized dose painting plan is used in Figs. 1 and 2 and compared with the clinical treatment plan. The dose painting prescription function used is a linear function with a minimum dose prescription of 21 Gy and an integral mean dose boost of 3.15 Gy. The figures illustrate how calculations for typical SRS metrics that include nontarget voxels would be sensitive to choice of mean or minimum prescribed dose. The clinical plan has a single selectivity value of 0.70. Calculating selectivity for the dose painting plan using the mean gives 0.85, while using the minimum gives 0.74. Figure 2 also shows that although the absolute doses for dose painting may be higher than the higher prescription doses, as seen in the DVH, the optimization was able to keep these doses closer to 1 on the quality ratio and thus close to the prescribed values, as seen in the QVH.

Figure 3 shows the correlation coefficients between all used metrics, where the data are combined from all 8 cases and all prescription functions. In all metrics except QF_{cold} and GI, a higher value is desirable, and the

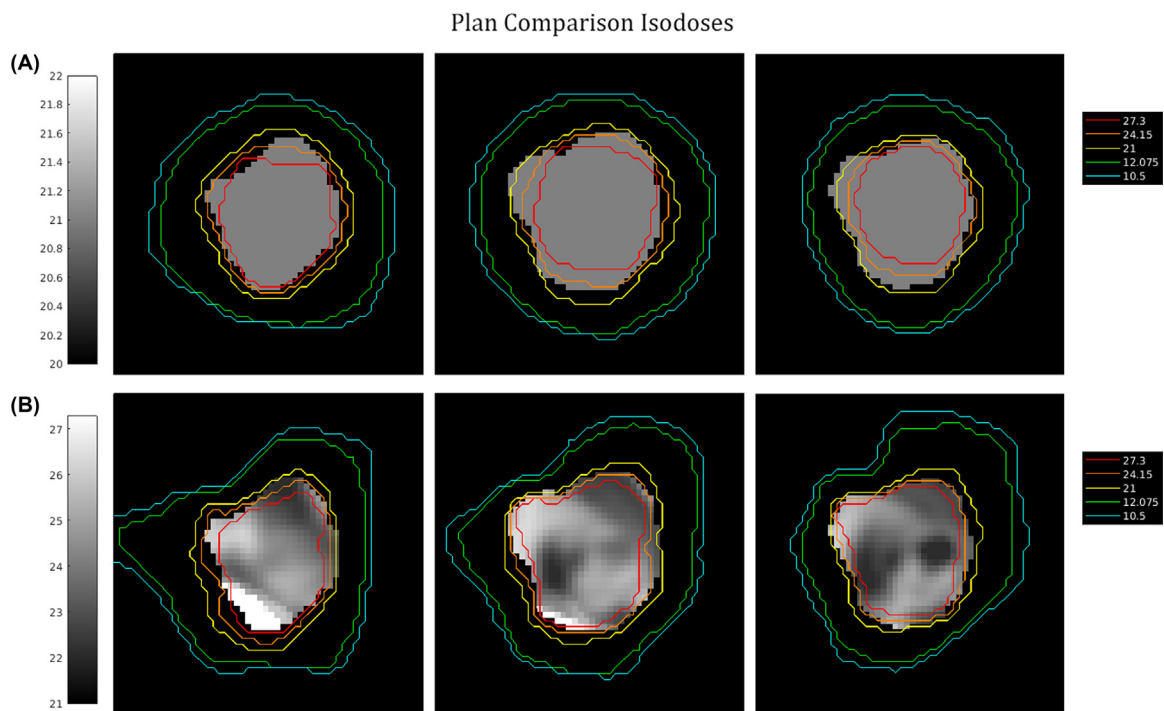


Figure 1 Example isodose lines to illustrate the differences in calculating using minimum or mean. (A) A clinical plan with a single prescription of 21 Gy. (B) A dose painting plan with minimum and mean prescriptions of 21 and 24.15 Gy, respectively. The voxel color indicates the prescribed dose, and isodose lines are based on the treatment plan dose.

magnitude of correlation is of most significance. The 4 strongly correlated groups are indicative of the focus of each set of metrics: (1) metrics that focus on target voxels (Coverage*, $D_{95\%}$ *, $V_{95\%}$ *, QF_{cold}), (2) metrics that focus on or are dominated by target overdose (QF_{hot} , $QF_{hot,150\%}$, QF , IDR), (3) metrics that focus on the voxels

in the near vicinity of the target (selectivity, PCI), and (4) metrics that focus on an extended volume beyond near the target (GI, EI).

QF_{hot} and $QF_{hot,150\%}$ have strong correlation to QF , showing a clear domination of QF by apparent target overdose when used to study SRS plans. There is a

Plan Comparison Histograms

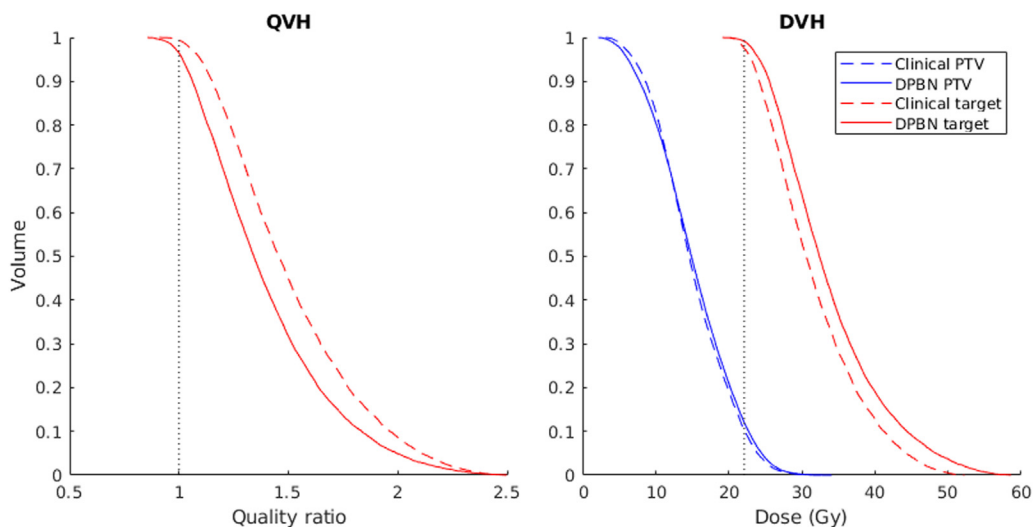


Figure 2 Example histograms to illustrate the differences in assessments for clinical single-dose prescriptions and for dose painting by numbers prescriptions. The quality volume histograms and dose volume histograms are for the target and planning target volume surrounding the target.

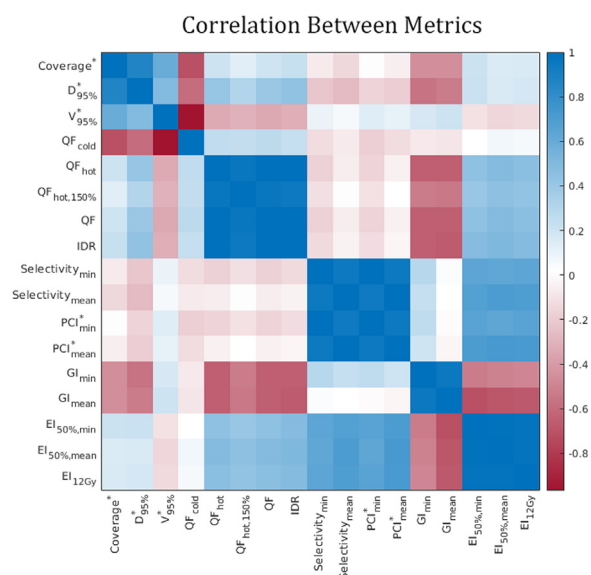


Figure 3 Correlation matrix for applicable assessment metrics.

noticeable correlation between these 4 metrics and GI, which aligns with the expectation that as the target dose is increased, dose fall-off gets steeper.

Selectivity and PCI are expectedly closely correlated as PCI is a product of coverage and selectivity, especially as coverages for all our example cases are close to 1. GI and EI use similar volumes and are similarly correlated.

Figure 4 shows a closer comparison between modified SRS metrics, PCI*_{min} and PCI*_{mean}, GI_{min} and GI_{mean}, and EI_{min} and EI_{mean}. The data are taken from all cases, prescription functions, and dose boost levels. Overall, the grouping of data points shows that these metrics are largely determined by case.

In Fig. 4A, the separation between the metrics grows as boost level increases, where the trendlines move increasingly further from the $x = y$ line. In Fig. 4B and 4C, boost level does not have as clear an effect on metric choice, with trendlines closer to the $x = y$ line and to each other.

Figure 5 explores the use of 2 metrics modified from QF to quantify target overdose. The ideal value of QF for dose painting radiation therapy plans is zero, and QF_{hot}, which only calculates for overdose, never reaches zero for either clinical or dose painting SRS plans. QF_{hot,150%} only calculates for overdose exceeding 150% and does reach zero in some SRS plans. There is no clear trend for dose boost level and some clustering of points for cases 06 and 07.

Discussion

The groups of correlated metrics show there is some flexibility for clinicians to use metrics to provide the most insight for their study.

The strong correlation between each pair of mean- and minimum-oriented metrics for selectivity, PCI, GI, and EI show that we may pick the most suitable focus depending on the study. For example, with studies using integral boost prescription functions where the mean prescription is predetermined, mean-oriented metrics would be more comparable between plans. On the other hand, studies using the max boost method would have a mean prescription based on the set maximum boost, prescription function, and distribution of voxel image intensities, so it may be more appropriate to use minimum-oriented metrics.

The comparisons in Fig. 4 characterize the differences one might expect when choosing between the 2 sets of metrics, and this could be an additional consideration when choosing the type of dose painting boost. The trendlines for PCI*_{mean} and PCI*_{min} indicate that the choice would have noticeable effect on the metric's value, whereas for GI and EI, which are calculated using volumes beyond the immediate vicinity of targets, the choice between mean- or minimum-oriented metric has less effect. It may also be a consideration to choosing EI over GI, with the lower variation due to consideration of dose in the whole volume and not just the size of the volume, as well as the numerator of integral target dose being unaffected by choice of mean or minimum prescription dose. Further advantages of EI are explored in the study by Dimitriadis and Paddick.⁴⁹ Nonetheless, either mean- or minimum-oriented metrics would allow clinical interpretations similar to existing SRS metrics and if applied to single-prescription plans would give the same values as existing metrics.

For target underdose metrics, QF_{cold} and V_{95%*} have a strong correlation, indicating that V_{95%*}, modified from the widely used V_{95%}, could sufficiently cover underdose concerns of the dose painting. Coverage* and D_{95%*} may also continue to be used as primary indications of underdose levels in dose painting plans.

For overdose metrics, the strong correlation between QF_{hot} and QF, together with the weak correlation between QF_{cold} and QF, indicate that QF alone cannot be applied to dose painting in SRS, as the high apparent overdose levels overshadow the small levels of underdose. Using QF_{hot,150%} instead of QF_{hot} extends the acceptable dose to 150% of prescribed dose, and this relative threshold may be adjusted depending on case or study. Furthermore, the possibility of QF_{hot,150%} reaching zero aligns with the current ideal of QF in assessing radiation therapy plans. Clinicians familiar with the prior use of QF in dose painting radiation therapy have the option to use the separate metrics QF_{cold} and QF_{hot} or QF_{hot,150%}.

On the other hand, integral dose is a known concept in radiation therapy, and IDR uses integral dose, like the existing SRS metric EI. The strong correlation between IDR and QF_{hot} or QF_{hot,150%} shows that IDR may also be used as an indication of the amount of overdose.

Metric Comparisons: Mean vs. Minimum

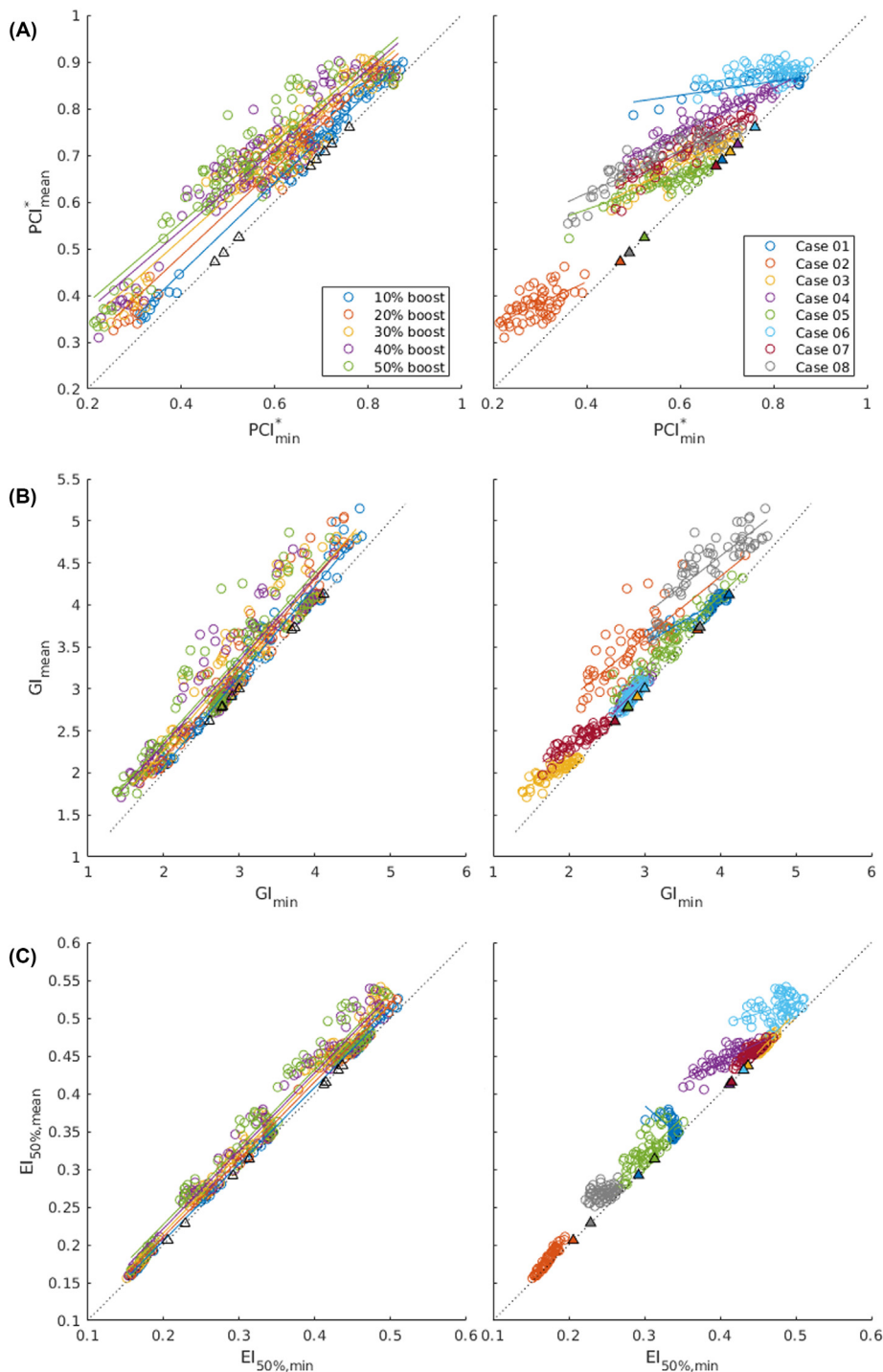


Figure 4 Comparison between mean- and minimum-oriented metrics for (A) Paddick conformity index, (B) gradient index, and (C) efficiency index calculated for dose painting plans, with clinical plans marked in \triangle . The data set is separated by dose painting dose boost level and by case to illustrate the effect on each metric.

Regarding the effect of prescription functions in dose painting, the use of different prescription functions in this study allows the creation of a variety of dose painting prescriptions from the available cases and images and thus

allows us to apply the investigation of metrics to various types of plans. The effect of prescription function on plan quality, and thus metric values, may be explored in future work.

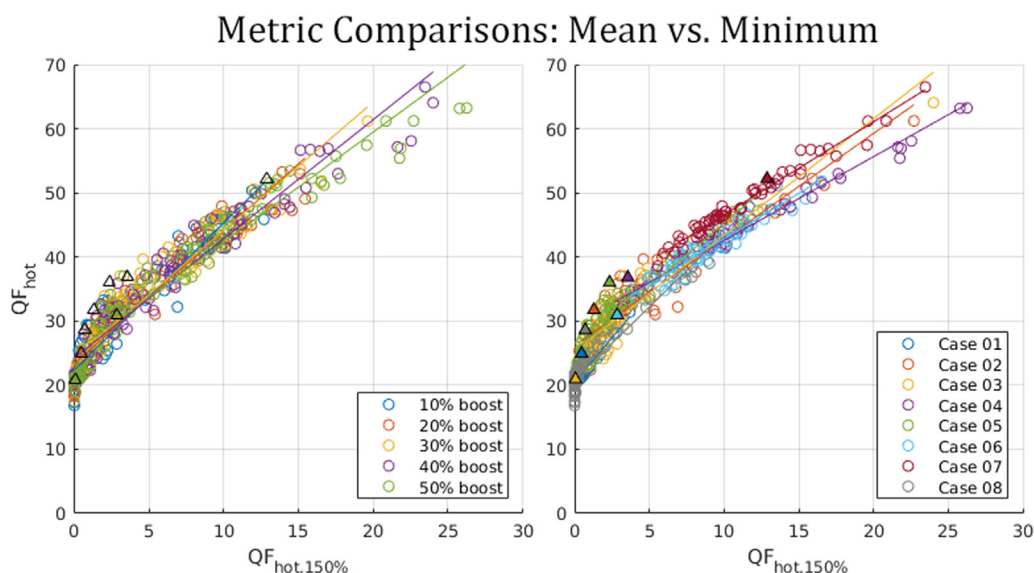


Figure 5 Comparison between quality factor (QF)_{hot} and $QF_{hot,150\%}$, with clinical plans marked in Δ .

Conclusion

Using metrics modified from existing SRS or dose painting metrics is demonstrated to be possible, with the modified metrics accounting for the characteristics of dose painting SRS plans. Users familiar with existing SRS single prescription metrics may easily adopt the modified versions of coverage, selectivity, PCI, GI, and EI, as they would give values equal to the original metrics when applied to single prescription plans. Users familiar with QF in dose painting radiation therapy may apply the separate metrics of QF_{cold} and QF_{hot} for dose painting SRS.

The combined use of mean- and minimum-oriented metrics would give the most information to users, but using 1 set that fits the dose painting boost method, integral boost, or max boost would be sufficient to allow comparison between plans and cases.

Dose histograms (DVH and QVH) and dose distribution visualizations remain useful for dose painting SRS plans and complement the use of any used metrics.

Disclosures

Håkan Nordström and Nelly Nygren are employees of Elekta Instrument AB.

Supplementary materials

Supplementary material associated with this article can be found in the online version at [doi:10.1016/j.adro.2023.101281](https://doi.org/10.1016/j.adro.2023.101281).

References

- Barragán AM, Differding S, Janssens G, Lee JA, Sterpin E. Feasibility and robustness of dose painting by numbers in proton therapy with contour-driven plan optimization. *Med Phys*. 2015;42:2006-2017.
- Bentzen SM. Theragnostic imaging for radiation oncology: Dose-painting by numbers. *Lancet Oncol*. 2005;6:112-117.
- Alber M, Paulsen F, Eschmann SM, Machulla HJ. On biologically conformal boost dose optimization. *Phys Med Biol*. 2003;48:N31-N35.
- Thorwarth D, Eschmann SM, Paulsen F, Alber M. Hypoxia dose painting by numbers: A planning study. *Int J Radiat Oncol Biol Phys*. 2007;68:291-300.
- Madani I, Duprez F, Boterberg T, et al. Maximum tolerated dose in a phase I trial on adaptive dose painting by numbers for head and neck cancer. *Radiother Oncol*. 2011;101:351-355.
- Differding S, Sterpin E, Janssens G, Hanin FX, Lee JA, Grégoire V. Methodology for adaptive and robust FDG-PET escalated dose painting by numbers in head and neck tumors. *Acta Oncol*. 2016;55:217-225.
- Arnesen MR, Knudtsen IS, Rekestad BL, et al. Dose painting by numbers in a standard treatment planning system using inverted dose prescription maps. *Acta Oncol*. 2015;54:1607-1613.
- van Schie MA, Steenbergen P, Dinh CV, et al. Repeatability of dose painting by numbers treatment planning in prostate cancer radiotherapy based on multiparametric magnetic resonance imaging. *Phys Med Biol*. 2017;62:5575-5588.
- Wright P, Arnesen MR, Lønne PI, et al. Repeatability of hypoxia dose painting by numbers based on EF5-PET in head and neck cancer. *Acta Oncol*. 2021;60:1386-1391.
- Meijer G, Steenhuisen J, Bal M, De Jaeger K, Schuring D, Theuvs J. Dose painting by contours versus dose painting by numbers for stage II/III lung cancer: Practical implications of using a broad or sharp brush. *Radiother Oncol*. 2011;100:396-401.
- Berwouts D, Olteanu LAM, Duprez F, et al. Three-phase adaptive dose-painting-by-numbers for head-and-neck cancer: Initial results of the phase I clinical trial. *Radiother Oncol*. 2013;107:310-316.
- Grönlund E, Johansson S, Montelius A, Ahnesjö A. Dose painting by numbers based on retrospectively determined recurrence probabilities. *Radiother Oncol*. 2017;122:236-241.

13. Duprez F, De Neve W, De Gerssem W, Coghe M, Madani I. Adaptive dose painting by numbers for head-and-neck cancer. *Int J Radiat Oncol Biol Phys.* 2011;80:1045-1055.
14. Dirscherl T, Rickhey M, Bogner L. Feasibility of TCP-based dose painting by numbers applied to a prostate case with 18F-choline PET imaging. *Z Med Phys.* 2012;22:48-57.
15. Sterpin E, Differding S, Janssens G, Geets X, Grégoire V, Lee JA. Generation of prescriptions robust against geometric uncertainties in dose painting by numbers. *Acta Oncol.* 2015;54:253-260.
16. Witte M, Shakirin G, Houweling A, Peulen H, van Herk M. Dealing with geometric uncertainties in dose painting by numbers: Introducing the ΔVH . *Radiother Oncol.* 2011;100:402-406.
17. Grönlund E, Almhagen E, Johansson S, Traneus E, Ahnesjö A. Robust maximization of tumor control probability for radicality constrained radiotherapy dose painting by numbers of head and neck cancer. *Phys Imaging Radiat Oncol.* 2019;12:56-62.
18. Lippitz B, Lindquist C, Paddick I, Peterson D, O'Neill K, Beaney R. Stereotactic radiosurgery in the treatment of brain metastases: The current evidence. *Cancer Treat Rev.* 2014;40:48-59.
19. Shaw E, Kline R, Gillin M, et al. Radiation therapy oncology group: Radiosurgery quality assurance guidelines. *Int J Radiat Oncol Biol Phys.* 1993;27:1231-1239.
20. Chen JC, Girvigian MR. Stereotactic radiosurgery: Instrumentation and theoretical aspects—part 1. *Perm J.* 2005;9:23.
21. Gevaert T, Verellen D, Tournel K, et al. Setup accuracy of the Novalis ExacTrac 6DOF system for frameless radiosurgery. *Int J Radiat Oncol Biol Phys.* 2012;82:1627-1635.
22. Ramakrishna N, Rosca F, Friesen S, Tezcanli E, Zygmanski P, Hacker F. A clinical comparison of patient setup and intra-fraction motion using frame-based radiosurgery versus a frameless image-guided radiosurgery system for intracranial lesions. *Radiother Oncol.* 2010;95:109-115.
23. Opp D, Feygelman V, Sarangkasiri S, et al. Pre-treatment simulation of target motion for frameless intracranial stereotactic radiosurgery treatments using the Novalis ExacTrac system. *Int J Radiat Oncol Biol Phys.* 2009;75:S602.
24. Duggar WN, Morris B, Fatemi A, et al. Gamma Knife® Icon CBCT offers improved localization workflow for frame-based treatment. *J Appl Clin Med Phys.* 2019;20:95-103.
25. Zeverino M, Jaccard M, Patin D, et al. Commissioning of the Leksell Gamma Knife® Icon™. *Med Phys.* 2017;44:355-363.
26. Chung HT, Park WY, Kim TH, Kim YK, Chun KJ. Assessment of the accuracy and stability of frameless gamma knife radiosurgery. *J Appl Clin Med Phys.* 2018;19:148-154.
27. Wright G, Harrold N, Hatfield P, Bownes P. Validity of the use of nose tip motion as a surrogate for intracranial motion in mask-fixed frameless Gamma Knife® Icon™ therapy. *J Radiosurg SBRT.* 2017;4:289-301.
28. Sarfehnia A, Ruschin M, Chugh B, et al. Performance characterization of an integrated cone-beam CT system for dedicated gamma radiosurgery. *Med Phys.* 2018;45:4179-4190.
29. Ghazal M, Fager M, Samadi A, Gubanski M, Benmakhlouf H. On the stability of Leksell Vantage stereotactic head frame fixation in Gamma Knife radiosurgery: A study based on cone-beam computed tomography imaging and the High Definition Motion Management system. *J Neurosurg.* 2023;1-9.
30. Carminucci A, Nie K, Weiner J, Hargreaves E, Danish SF. Assessment of motion error for frame-based and noninvasive mask-based fixation using the Leksell Gamma Knife Icon radiosurgery system. *J Neurosurg.* 2018;129(Suppl1):133-139.
31. Bush A, Vallow L, Ruiz-Garcia H, et al. Mask-based immobilization in Gamma Knife stereotactic radiosurgery. *J Clin Neurosci.* 2021;83:37-42.
32. Grimm MA, Köppen U, Stieler F, et al. Prospective assessment of mask versus frame fixation during Gamma Knife treatment for brain metastases. *Radiother Oncol.* 2020;147:195-199.
33. Chung HT, radiosurgery Lee DJ. Stereotactic. *Prog Med Phys.* 2020;31:63-70.
34. Torrens M, Chung C, Chung HT, et al. Standardization of terminology in stereotactic radiosurgery: Report from the Standardization Committee of the International Leksell Gamma Knife Society: Special topic. *J Neurosurg.* 2014;121(Suppl 2):2-15.
35. Olteanu LA, Berwouts D, Madani I, et al. Comparative dosimetry of three-phase adaptive and nonadaptive dose-painting IMRT for head-and-neck cancer. *Radiother Oncol.* 2014;111:348-353.
36. Park YK, Park S, Wu HG, Kim S. A new plan quality index for dose painting radiotherapy. *J Appl Clin Med Phys.* 2014;15:316-325.
37. Vanderstraeten B, Duthoy W, De Gerssem W, De Neve W, Thierens H. [18F] fluoro-deoxy-glucose positron emission tomography ([18F] FDG-PET) voxel intensity-based intensity-modulated radiation therapy (IMRT) for head and neck cancer. *Radiother Oncol.* 2006;79:249-258.
38. Podgorsak EB, Pace GB, Olivier A, Pla M, Souhami L. Radiosurgery with high energy photon beams: A comparison among techniques. *Int J Radiat Oncol Biol Phys.* 1989;16:857-865.
39. Coolens C, Driscoll B, Foltz W, Svistoun I, Sinno N, Chung C. Unified platform for multimodal voxel-based analysis to evaluate tumour perfusion and diffusion characteristics before and after radiation treatment evaluated in metastatic brain cancer. *Br J Radiol.* 2019;92: 20170461.
40. Winter JD, Moraes FY, Chung C, Coolens C. Detectability of radiation-induced changes in magnetic resonance biomarkers following stereotactic radiosurgery: A pilot study. *PLOS One.* 2018;13: e0207933.
41. Farjam R, Tsien CI, Feng FY, et al. Investigation of the diffusion abnormality index as a new imaging biomarker for early assessment of brain tumor response to radiation therapy. *Neuro-Oncol.* 2014;16:131-139.
42. Press RH, Shu HK, Shim H, et al. The use of quantitative imaging in radiation oncology: A quantitative imaging network (QIN) perspective. *Int J Radiat Oncol Biol Phys.* 2018;102:1219-1235.
43. Søvik Å, Malinen E, Bruland ØS, Bentzen SM, Olsen DR. Optimization of tumour control probability in hypoxic tumours by radiation dose redistribution: A modelling study. *Phys Med Biol.* 2006;52:499-513.
44. Das SK, Miften MM, Zhou S, et al. Feasibility of optimizing the dose distribution in lung tumors using fluorine-18-fluorodeoxyglucose positron emission tomography and single photon emission computed tomography guided dose prescriptions. *Med Phys.* 2004;31:1452-1461.
45. Bowen SR, Flynn RT, Bentzen SM, Jeraj R. On the sensitivity of IMRT dose optimization to the mathematical form of a biological imaging-based prescription function. *Phys Med Biol.* 2009;54:1483-1501.
46. Bentzen SM, Grégoire V. Molecular imaging—based dose painting: A novel paradigm for radiation therapy prescription. *Semin Radiat Oncol.* 2011;21:101-110.
47. Oskoorouchi MR, Ghaffari HR, Terlaky T, Aleman DM. An interior point constraint generation algorithm for semi-infinite optimization with health-care application. *Operation Res.* 2011;59:1184-1197.
48. Paddick I, Lippitz B. A simple dose gradient measurement tool to complement the conformity index. *J Neurosurg.* 2006;105(Supplement):194-201.
49. Dimitriadis A, Paddick I. A novel index for assessing treatment plan quality in stereotactic radiosurgery. *J Neurosurg.* 2018;129(Suppl1):118-124.
50. Paddick I. A simple scoring ratio to index the conformity of radiosurgical treatment plans. *J Neurosurg.* 2000;93(Supplement 3):219-222.